J|A|C|S
COMMUNICATIONS

Pore Space Partition and Charge Separation in Cage-within-Cage Indium−Organic Frameworks with High CO_2 Uptake

Shou-Tian Zheng,[†] Julia T. Bu,[‡,§] Yufei Li,[†] Tao Wu,[‡] Fan Zuo,[‡] Pingyun Feng,*[,‡] and Xianhui Bu*[,†]

Department of Chemistry and Biochemistry, California State University, Long Beach, California 90840, United States, and Department of Chemistry, University of California, Riverside, California 92521, United States

Received August 2, 2010; E-mail: xbu@csulb.edu; pingyun.feng@ucr.edu

Abstract: The integration of negatively charged single-metal building blocks $\{In(CO_2)_4\}$ and positively charged trimeric clusters $\{In_3O\}$ leads to three unique cage-within-cage-based porous materials, which exhibit not only high hydrothermal, thermal, and photochemical stability but also attractive structural features contributing to a very high CO_2 uptake capacity of up to 119.8 L/L at 273 K and 1 atm.

Crystalline porous materials are an important class of materials due to their large-scale industrial applications in heterogeneous catalysis, gas separation, and so on.[1,2] In recent years, there has been an intensive effort aimed at the design of new generations of porous materials that can be used as high-capacity adsorbents for gas storage and delivery or CO_2 sequestration.[3−5] Among many different types of materials studied for such purposes, metal−organic framework materials (MOFs) have emerged as one of the favorites because of their compositional and geometric tunability and very high surface areas.[6,7]

It has been recognized that high surface area and large pore volume do not necessarily lead to a high uptake capacity for small molecules such as CO_2, especially under ambient conditions. Recent studies have indicated several features that are desirable for enhancing storage capacity of small gas molecules.[8−10] One such feature is the suitable pore size commensurate with the size of a gas molecule. This makes it necessary to develop synthetic strategies to generate a pore architecture that allows for efficient use of the pore space, for example, through pore space partitioning of large cage structures using methods such as impregnation and catenation. Another factor currently receiving considerable attention is the generation of individual localized binding sites using methods such as (1) creation of coordinatively unsaturated metal sites (also called open-metal sites) located on either inorganic nodes or organic linkers (or as extraframework species, like Li^+ in zeolite X) and (2) use of organic linkers with functional groups such as $-NH_2$.[4] Furthermore, the solid−gas interactions can also be enhanced using a somewhat delocalized approach through the generation of the electric field across the pore space that is capable of polarizing gas molecules and increasing their interaction with charged internal pore surfaces or charged extraframework species.[11] However, this latter approach is far less well studied experimentally because the vast majority of MOFs have an electrically neutral framework.

Here we report three interesting cage-within-cage porous In−carboxylate frameworks $[(CH_3)_2NH_2][In_3O(BTC)_2(H_2O)_3]_2[In_3(BTC)_4]\cdot 7DMF\cdot 23H_2O$ (denoted as CPM-5, CPM = crystalline porous materials), $[(CH_3)_2NH_2][In_3O(BTC)_2(H_2O)_3]_2[In(BTC)_{4/3}][In(BTC)_{4/3}(H_2O)]_2\cdot$solvent (CPM-5′), and $[CH_3NH_3][In_3O(BTC)_2(H_2O)_3]_2[In_3(BTC)_4]\cdot$solvent (CPM-6, BTC = 1,3,5-benzenetricarboxylate) that integrate several aforementioned features (e.g., pore size partition, charged frameworks, and open metal sites) and exhibit high CO_2 uptake capacity. CPM-5 crystallizes in a highly symmetric and yet noncentrosymmetric cubic space group $I\bar{4}3m$. As shown in Figure 1e, its most fascinating topological feature is the cage-within-cage structure in which a large Archimedean cage (truncated octahedral cage, also called sodalite cage, denoted as the In_{24} cage here) encapsulates a small Archimedean cage (truncated tetrahedral cage, denoted as the In_{12} cage here). The outer sodalite cage is

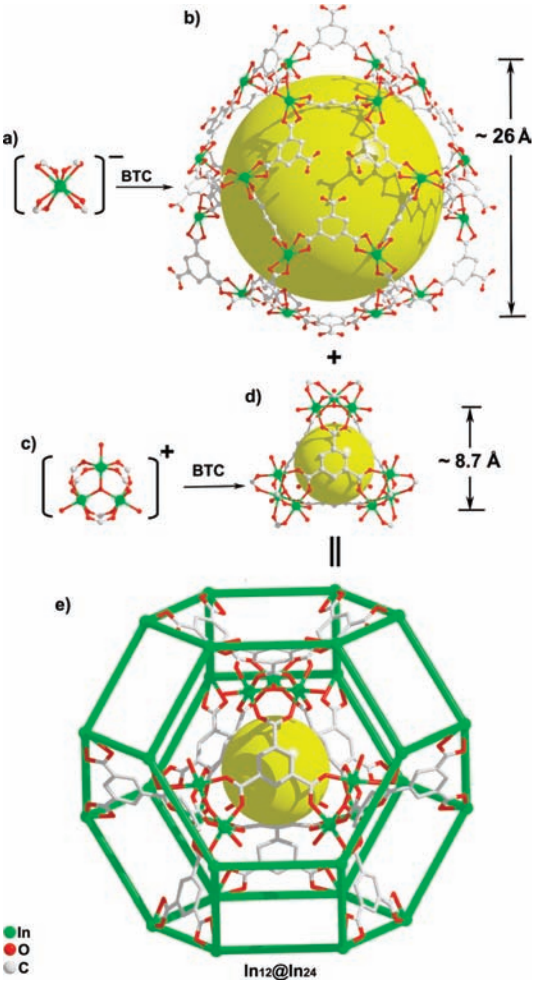

Figure 1. (a−e) Structures of monomeric In^{3+} ion, In_{24} cage, trimeric $\{(In_3O)(H_2O)_3\}$ unit, In_{12} cage, and $In_{12}@In_{24}$ cage, respectively. The green solid lines represent BTCs.

[†] California State University, Long Beach.
[‡] University of California, Riverside.
[§] Research Intern from J. W. North High School, Riverside.

10.1021/ja106903p

formed by 24 mononuclear In^{3+} sites, each of which is eight-coordinated to oxygen atoms, but serves as a four-connected node because of the formation of the chelate bond (Figure 1a). Any two adjacent In^{3+} sites on the In_{24} cage are bridged by a BTC^{3-} anion using two of its three carboxylic groups, forming a sodalite cage (Figure 1b) that is significantly larger than other MOFs with a sodalite topology such as ZIF-8 and sod-ZMOF (Table S1).[6b,12] The third carboxylic group of each BTC serves to interconnect the outer In_{24} cage with the inner In_{12} cage (Figure 1e).[13a] The In_{12} cage is built from four trimeric $\{(In_3O)(H_2O)_3\}$ clusters which are joined together by four BTCs into a truncated tetrahedron $\{[In_3(H_2O)_3(\mu_3\text{-}O)]_4(BTC)_4\}$ (Figures 1c, 1d).

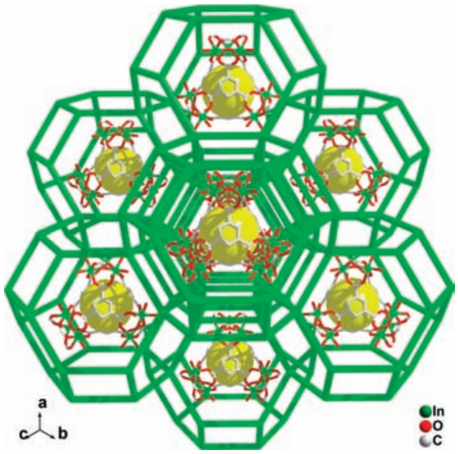

Figure 2. View of the 3D structure of CPM-5. Some BTC ligands interconnecting In_{12} and In_{24} cages are omitted for clarity.

The overall 3D structure can be understood as a body-centered cubic packing of the larger In_{24} cages, each of which contains one In_{12} cage at the center (Figure 2). Although a number of metal−organic polyhedral frameworks have been reported,[13,14] so far there are few examples of the cage-within-cage-based 3D polyhedral framework. The formation of the core−shell-type $In_{12}@In_{24}$ 3D structure has the potential to enhance sorption properties of small gas molecules such as CO_2. First, the In_{24} cage which is about 25.7 × 25.7 × 25.7 $Å^3$ in dimension is far too large for the storage of small gas molecules. The interconnection between the In_{12} cage (dimension ∼0.9 nm) and the In_{24} cage (∼2.5 nm) (Figure 1c) by 12 BTCs serves to partition the pore space of the large sodalite cage into multiple domains with the pore radius in the range of 4.00−1.68 Å (volume: 268−19.9 $Å^3$) (Table S2).[15] Even with the small In_{12} cage within the In_{24} cage and the BTC interconnectors between In_{12} and In_{24} cages, CPM-5 still possesses a relatively large guest-accessible volume of 8141 $Å^3$ per unit cell (47.9% of the total unit cell volume). The formation of the cage-within-cage structure is related to two distinctly different In^{3+} configurations: a monomeric four-connected $[In(O_2CR)_4]^-$ site and trimeric $[In_3(O)(O_2CR)_6(H_2O)_3]^+$ clusters. Currently, the design and synthesis of single metal-based zeolite-*like* MOFs or MBB-based (MBB = molecular building block) porous MOFs are two active areas. In comparison, MOFs that integrate both single-metal and metal-cluster building units are less well-known and represent a fruitful route for the design of novel porous materials. In CPM-5, both single metal $\{In(O_2CR)_4\}$ units and the trimeric $\{In_3(O)(O_2CR)_6(H_2O)_3\}$ MBBs are present. Since the In/COO^- ratio in the structure differs greatly depending on whether the indium sites exist in the monomeric form or trimeric forms, a systematic synthetic exploration of the In/COO^- ratio represents a viable strategy for the selection of the desired In form, even if the In/COO^- ratio in the crystal structures does not necessarily correspond to a particular range of In/COO^- ratios in the synthesis mixture. It is of particular interest that the outer cage made from single metal $\{In(O_2CR)_4\}$ units is negatively charged whereas the inner cage made from trimeric $\{In_3(O)(O_2CR)_6(H_2O)_3\}$ MBBs is positively charged, leading to an electric field within the shell region between In_{24} and In_{12} cages. In addition to the pore space partitioning and the electric field effect associated with the cage-within-cage architecture, CPM-5 integrates another desirable feature, open metal sites. Attached to each indium ion of the inner In_{12} cage (67% of all indium sites in CPM-5) is a dangling water ligand which upon removal serves to generate open In^{3+} sites, as supported by IR spectra of the CPM-5 sample before and after degassing (Figure S4).

A large quantity of pure CPM-5 (gram-scale) can be readily prepared. Powder X-ray diffraction (PXRD) indicates CPM-5 is stable in water at room temperature and remains highly crystalline even after being in boiling water for 8 h (Figure S5). Furthermore, CPM-5 is stable photochemically and retains its crystallinity after exposure to strong UV radiations for 10 h (Figure S6). Thermogravimetric analysis of CPM-5 shows that the removal of solvent molecules occurs in the temperature range of 40−230 °C and no further weight loss up to 300 °C (Figure S7). PXRD further confirms that the desolvated sample retains its crystallinity up to about 320 °C (Figure S8).

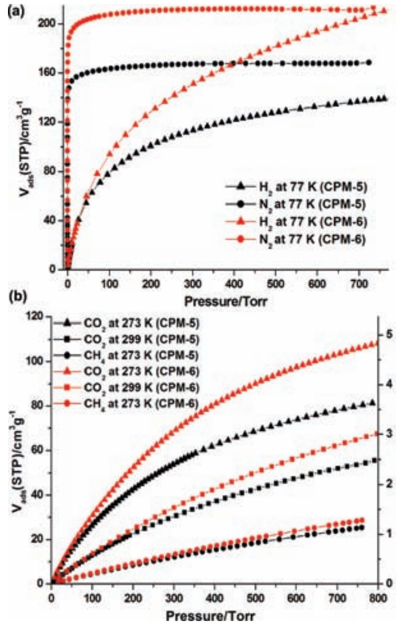

Figure 3. (a) N_2 and H_2 adsorption isotherms of CPM-5 and CPM-6. (b) CO_2 and CH_4 adsorption isotherms of CPM-5 and CPM-6.

Interestingly, CPM-5′, a tetragonal variation of cubic CPM-5, can be prepared in the presence of 4,4′-bipyridine (Figure S9). The only difference between CPM-5 and CPM-5′ is in the coordination of the monomeric indium site on the outer In_{24} cage. In CPM-5, H_2O only attaches to the inner In_{12} cage whereas, in CPM-5′, two-thirds of In^{3+} sites on the In_{24} cage are also bonded to H_2O (in addition to H_2O on the In_{12} cage). PXRD shows that CPM-5′ can be converted to CPM-5 after H_2O on the In_{24} cage is removed at 230 °C (Figure S10).

Hydrothermal, thermal, and photochemical stability, coupled with open indium sites, pore space partitioning, and favorable charge separation in CPM-5 render it a good candidate for the study of gas sorption properties. The measurements (N_2, H_2, CH_4, and CO_2)

were performed on a Micromeritics ASAP 2020 surface-area and pore-size analyzer. No sample activation was applied, and the as-synthesized sample was directly degassed at 230 °C for 48 h under vacuum prior to the measurement. CPM-5 exhibits a type I adsorption isotherm typical of materials of permanent microporosity (Figure 3a). The Langmuir and BET surface areas were 733 and 580 m^2/g, respectively. A micropore volume of 0.258 cm^3/g (using Horvath−Kawazoe method) and the median pore size of 4.89 Å were also calculated. The small pore size is clearly the effect of the pore size partition resulting from the unique In_{12}@In_{24} topology.

CPM-5 exhibits a very high CO_2 uptake capacity of 81.3 cm^3/g (91.3 L/L) at 273 K and 1 atm (Figure 3b). At room temperature (299 K) and 1 atm, CPM-5 has a CO_2 uptake of 54.5 cm^3/g (61.2 L/L). It is worth noting that even though numerous MOF structures have been reported, few exhibit a CO_2 uptake of more than 60 L/L at 298 K and 1 atm.[4c,16,17] Clearly, the unique structural factors of CPM-5 described above contribute significantly to its high CO_2 uptake. For H_2 gas, the adsorption isotherms revealed that CPM-5 can adsorb 139.2 cm^3/g of H_2 (1.24 wt %) at 77 K and 1 atm.

To further improve the gas uptake capacity, we also varied the size of extraframework organic cations and prepared an isostructural compound CPM-6 with smaller organic cations ($CH_3NH_3^+$, Figure S11). As expected, CPM-6 exhibits significantly improved gas sorption properties. While the improvement in the surface area is moderate (the Langmuir and BET surface areas of CPM-6 are 931 and 596 m^2/g, respectively), the CO_2 and H_2 uptake capacities of CPM-6 are remarkably enhanced (for CO_2 at 1 atm: 106.7 cm^3/g (119.8 L/L) at 273 K and 65 cm^3/g (73 L/L) at 299 K; for H_2 at 1 atm: 210.6 cm^3/g (1.88 wt %) at 77 K). In comparison, the adsorption of CH_4 gas on both CPM-5 and CPM-6 are markedly lower than that of CO_2. At 273 K, the CO_2/CH_4 ratios of uptake are ca. 7.5−3.2 between 0.01 and 1 bar.

In conclusion, the integration of negatively charged single-metal building blocks $\{In(CO_2)_4\}$ and positively charged trimeric clusters $\{In_3O\}$ leads to an exceptional porous material in which the large In_{24} sodalite cage encapsulates and interconnects a small In_{12} cage laden with open In^{3+} sites. The cage-within-cage architecture partitions the pore space into small charge-separated domains that are among key desirable features needed for enhanced gas sorption through a better size match and stronger charged-induced forces. These integrated structural features (i.e., open metal sites, pore size partition, and electric field) contribute to a very high CO_2 uptake capacity. Furthermore, the material exhibits a high hydrothermal, thermal, and photochemical stability.

Acknowledgment. We thank the support of this work by the NSF (X.B., DMR-0846958) and DOE (P.F., ER46631; DE-SC0002235). X.B. is a Henry Dreyfus Teacher Scholar.

Supporting Information Available: Experimental details, TGA, XRPD, EA, IR, and additional figures. This material is available free of charge via the Internet at http://pubs.acs.org.

References

(1) (a) Xiao, B.; Byrne, P. J.; Wheatley, P. S.; Wragg, D. S.; Zhao, X.; Fletcher, A. J.; Thomas, K. M.; Peters, L.; Evans, J. S. O.; Warren, J. E.; Zhou, W.; Morris, R. E. *Nat. Chem.* **2009**, *1*, 289. (b) Phan, A.; Doonan, C. J.; Uriberomo, F. J.; Knobler, C. B.; O'Keefee, M.; Yaghi, O. M. *Acc. Chem. Res.* **2010**, *43*, 58–67. (c) Tanaka, D.; Henke, A.; Albrecht, K.; Moeller, M.; Nakagawa, K.; Kitagawa, S.; Groll, J. *Nat. Chem.* **2010**, *2*, 410–416. (d) Ma, L.; Falkowski, J. M.; Abney, C.; Lin, W. *Nat. Chem.* **2010**, *2*, 838–846.

(2) (a) Xiang, S.; Zhou, W.; Gallegos, J. M.; Liu, Y.; Chen, B. L. *J. Am. Chem. Soc.* **2009**, *131*, 12415–12419. (b) Li, K.; Olson, D. H.; Seidel, J.; Emge, T. J.; Gong, H.; Zeng, H.; Li, J. *J. Am. Chem. Soc.* **2009**, *131*, 10368–10369. (c) Lee, Y.; Farha, O. K.; Roberts, J.; Scheidt, K. A.; Nguyen, S. T.; Hupp, J. T. *Chem. Soc. Rev.* **2009**, *38*, 1450–1459.

(3) (a) Zhao, D.; Yuan, D.; Zhou, H. C. *Energy Environ. Sci.* **2008**, *1*, 222–235. (b) Sava, D. F.; Kravtsov, V. C.; Eckert, J.; Eubank, J. F.; Nouar, F.; Eddaoudi, M. *J. Am. Chem. Soc.* **2009**, *131*, 2864–10396. (c) Zheng, S.; Wu, T.; Zhang, J.; Chow, M.; Nieto, R. A.; Feng, P.; Bu, X. *Angew. Chem., Int. Ed.* **2010**, *49*, 5362–5366. (d) Hu, Y. H.; Zhang, L. *Adv. Mater.* **2010**, *22*, E117−E130.

(4) (a) An, J.; Fiorella, R. P.; Geib, S. J.; Rosi, N. L. *J. Am. Chem. Soc.* **2009**, *131*, 8401–8403. (b) An, J.; Rosi, N. L. *J. Am. Chem. Soc.* **2010**, *132*, 5578–5579. (c) Debatin, F.; Thomas, A.; Kelling, A.; Hedin, N.; Bacsik, Z.; Senkovska, I.; Kaskel, S.; Junginger, M.; Müller, H.; Schilde, U.; Jäger, C.; Friedrich, A.; Holdt, H. J. *Angew. Chem., Int. Ed.* **2010**, *49*, 1258–1262.

(5) (a) Morris, R. E.; Wheatley, P. S. *Angew. Chem., Int. Ed.* **2008**, *47*, 4966–4981. (b) Demessence, A.; D'Alessandro, D. M.; Foo, M. L.; Long, J. R. *J. Am. Chem. Soc.* **2009**, *131*, 8784–8786. (c) Banerjee, R.; Furukawa, H.; Britt, D.; Knobler, C.; O'Keeffe, M.; Yaghi, O. M. *J. Am. Chem. Soc.* **2009**, *131*, 3875–3877.

(6) (a) Férey, G. *Chem. Soc. Rev.* **2008**, *37*, 191–214. (b) Yuan, D.; Zhao, D.; Sun, D.; Zhou, H. C. *Angew. Chem., Int. Ed.* **2010**, *49*, 5357–5361. (c) Deng, H.; Doonan, C. J.; Furukawa, H.; Ferreira, R. B.; Towne, J.; Knobler, C. B.; Wang, B.; Yaghi, O. M. *Science* **2010**, *327*, 846–850.

(7) (a) Koh, K.; Wong-Foy, A. G.; Matzger, A. J. *J. Am. Chem. Soc*, **2009**, *131*, 4184–4185. (b) Zhao, D.; Yuan, D.; Sun, D.; Zhou, H. C. *J. Am. Chem. Soc.* **2009**, *131*, 9186–9188. (c) Furukawa, H.; Ko, N.; Go, Y. B.; Aratani, N.; Choi, S. B.; Choi, E.; Yazaydin, A. O.; Snurr, R. Q.; O'Keeffe, M.; Kim, J.; Yaghi, O. M. *Science* **2010**, *329*, 427–428.

(8) (a) Murray, L. J.; Dinca, M.; Long, J. R. *Chem. Soc. Rev.* **2009**, *38*, 1294–1314. (b) Han, S. S.; Mendoza-Cortés, J. L.; Goddard, W. A., III. *Chem. Soc. Rev.* **2009**, *38*, 1460–1476. (c) Xiang, S.; Zhou, W.; Zhang, Z.; Green, M. A.; Liu, Y.; Chen, B. *Angew. Chem., Int. Ed.* **2010**, *49*, 4615–4618.

(9) (a) Sava, D. F.; Kravtsov, V. C.; Eckert, J.; Eubank, J. F.; Nouar, F.; Eddaoudi, M. *J. Am. Chem. Soc.* **2009**, *131*, 10394–10396. (b) Ma, L.; Lin, W. *Angew. Chem., Int. Ed.* **2009**, *48*, 3637–3640. (c) Lin, J. B.; Zhang, J. P.; Chen, X. M. *J. Am. Chem. Soc.* **2010**, *132*, 6654–6656. (d) Farha, O. K.; Malliakas, C. D.; Kanatzidis, M. G.; Hupp, J. T. *J. Am. Chem. Soc.* **2010**, *132*, 950–952.

(10) (a) Dincã, M.; Long, J. R. *Angew. Chem., Int. Ed.* **2008**, *47*, 6766–6779. (b) Himsl, D.; Wallacher, D.; Hartmann, M. *Angew. Chem., Int. Ed.* **2009**, *48*, 4639–4642. (c) Mulfort, K. L.; Farha, O. K.; Stern, C. L.; Sarjeant, A. A.; Hupp, J. T. *J. Am. Chem. Soc.* **2009**, *131*, 3866–3868. (d) Ma, L.; Jin, A.; Xie, Z.; Lin, W. *Angew. Chem., Int. Ed.* **2009**, *48*, 9905–9908.

(11) (a) Düren, T.; Baeb, Y. S.; Snurr, R. Q. *Chem. Soc. Rev.* **2009**, *38*, 1237–1247. (b) Mavrandonakis, A.; Klontzas, E.; Tylianakis, E.; Froudakis, G. E. *J. Am. Chem. Soc.* **2009**, *131*, 13410–13414. (c) Higuchi, M.; Tanaka, D.; Horike, S.; Sakamoto, H.; Nakamura, K.; Takashima, Y.; Hijikata, Y.; Yanai, N.; Kim, J.; Kato, K.; Kubota, Y.; Takata, M.; Kitagawa, S. *J. Am. Chem. Soc.* **2009**, *131*, 10336–10337. (d) Yang, S.; Lin, X.; Blake, A. J.; Walker, G.; Hubberstey, P.; Champness, N. R.; Schröder, M. *Nat. Chem.* **2009**, *1*, 487–493.

(12) (a) Barea, E.; Navarro, J. A. R.; Salas, J. M.; Masciocchi, N.; Galli, S.; Sironi, A. *J. Am. Chem. Soc.* **2004**, *126*, 3014–3015. (b) Liu, Y.; Kravtsov, V. C.; Larsena, R.; Eddaoudi, M. *Chem. Commun* **2006**, 1488–1490. (c) Galli, S.; Masciocchi, N.; Tagliabue, G.; Sironi, A.; Navarro, J. A. R.; Salas, J. M.; Mendez-Liñan, L.; Domingo, M.; Perez-Mendoza, M.; Barea, E. *Chem.*−*Eur. J.* **2008**, *14*, 9890–9901.

(13) (a) Liu, Y.; Eubank, J. F.; Cairns, A. J.; Eckert, J.; Kravtsov, V. C.; Luebke, R.; Eddaoudi, M. *Angew. Chem., Int. Ed.* **2007**, *46*, 3278–3283. (b) Tranchmontagne, D. J.; Ni, Z.; O'Keeffe, M.; Yaghi, O. M. *Angew. Chem., Int. Ed.* **2008**, *47*, 5136–5147. (c) Zhao, D.; Yuan, D.; Sun, D.; Zhou, H. C. *J. Am. Chem. Soc.* **2009**, *131*, 9186–9188.

(14) (a) Chen, B.; Ockwig, N. W.; Millward, A. R.; Contreras, D. S.; Yaghi, O. M. *Angew. Chem., Int. Ed.* **2005**, *44*, 4745–4749. (b) Sava, D. F.; Kravtsov, V. C.; Nouar, F.; Wojtas, L.; Eubank, J. F.; Eddaoudi, M. *J. Am. Chem. Soc.* **2008**, *130*, 3766–3770. (c) Yan, Y.; Telepeni, I.; Yang, S.; Lin, X.; Kockelmann, W.; Dailly, A.; Blake, A. J.; Lewis, W.; Walker, G. S.; Allan, D. R.; Barnett, S. A.; Champness, N. R.; Schröder, M. *J. Am. Chem. Soc.* **2010**, *132*, 4092–4094.

(15) PLATON VOIDS probe diameter 1.2 Å: Spek, A. L. *J. Appl. Crystallogr.* **2003**, *36*, 7–13.

(16) Banerjee, R.; Phan, A.; Wang, B.; Knobler, C.; Furukawa, H.; O'Keeffe, M.; Yaghi, O. M. *Science* **2008**, *319*, 939.

(17) Alessandro, D. M. D.; Smit, B.; Long, J. R. *Angew. Chem., Int. Ed.* **2010**, *49*, 6058–6082.

JA106903P